



Contents lists available at ScienceDirect

Bioorganic & Medicinal Chemistry Letters

journal homepage: www.elsevier.com/locate/bmcl

Molecular modeling of a PAMAM-CGS21680 dendrimer bound to an A_{2A} adenosine receptor homodimer

Andrei A. Ivanov, Kenneth A. Jacobson *

Molecular Recognition Section, Laboratory of Bioorganic Chemistry, National Institute of Diabetes and Digestive and Kidney Diseases, National Institutes of Health, Bethesda, MD 20892, USA

ARTICLE INFO

Article history:

Received 22 May 2008

Revised 20 June 2008

Accepted 25 June 2008

Available online 28 June 2008

Keywords:

Nucleoside

G protein-coupled receptor

Dimerization

Homology modeling

Purines

Polymerbound drug

Functionalized congener

ABSTRACT

The theoretical possibility of bivalent binding of a dendrimer, covalently appended with multiple copies of a small ligand, to a homodimer of a G protein-coupled receptor was investigated with a molecular modeling approach. A molecular model was constructed of a third generation (G3) poly(amidoamine) (PAMAM) dendrimer condensed with multiple copies of the potent A_{2A} adenosine receptor agonist CGS21680. The dendrimer was bound to an A_{2A} adenosine receptor homodimer. Two units of the nucleoside CGS21680 could occupy the A_{2A} receptor homodimer simultaneously. The binding mode of CGS21680 moieties linked to the PAMAM dendrimer and docked to the A_{2A} receptor was found to be similar to the binding mode of a monomeric CGS21680 ligand.

Published by Elsevier Ltd.

G protein-coupled receptors (GPCRs) are transmembrane proteins which comprise a large and diverse superfamily of proteins. These receptors consist of seven transmembrane α -helices (TMs) connected by three extracellular and three intracellular loops. Besides the evidence that some GPCRs can function as monomeric units,¹ mounting evidence supports the critical functional role of homo- and heterodimerization and oligomerization of GPCRs.² It was shown that homo- and heterodimerized GPCRs display different pharmacological properties as compared with monomeric receptors.³

It was proposed that GPCR dimers can be activated or inhibited by bivalent ligands.⁴ In general, a bivalent ligand consists of two pharmacophore units connected by a spacer.⁵ Theoretically, but not necessarily, such bivalent ligands could occupy each of two units of a GPCR dimer simultaneously. Numerous studies have addressed the design of bivalent ligands for GPCRs, and several examples of potent bivalent ligands were reported for various receptors, including opioid, serotonin, muscarinic, and other receptors.^{6,7}

Recently, we have demonstrated that GPCRs can be activated not only by monomeric or bivalent ligands, but also by multivalent ligands. We have reported that intracellular signal transduction across the A_{2A} adenosine receptor (AR) can be induced by the A_{2A} AR agonist 2-[4-(2-carboxylethyl)phenylethylamino]-5'-N-ethyl-

carboxamidoadenosine (CGS21680 **1**) coupled covalently to a PAMAM dendrimer.⁸ A_{2A} AR agonists are known to display a potent antiaggregatory effect in human platelet preparations. Our functional assay clearly demonstrated a potent antiaggregatory effect of the PAMAM-CGS21680 dendrimer in human platelets.

However, there is no experimental evidence that CGS21680 units coupled to the PAMAM dendrimer can occupy more than one subunit of the A_{2A} AR simultaneously. In the present study, we utilize computational molecular modeling to investigate if the bivalent binding of PAMAM-CGS21680 to an A_{2A} AR dimer is theoretically allowed.

At the first stage, the molecular docking of CGS21680 **1** to the A_{2A} AR monomer was performed automatically with the Glide XP software.⁹ Our recently published molecular model of (*E*)-N-ethyl-1'-deoxy-1'-[6-amino-2-(5-phenyl-1-penten-1-yl)-9H-purin-9-yl]- β -D-ribofuranuronamide (2-phenylpentenyl-NECA) bound to the A_{2A} AR was utilized for the docking studies.¹⁰ The Protein Preparation Wizard of the MacroModel software¹¹ with its default parameters was used to prepare the model of the A_{2A} AR for the Glide calculations. The center of the box for the molecular docking of CGS21680 was placed in the center of 2-phenylpentenyl-NECA. The length of 28.44 Å was used for all box sides. Since the binding site of the initial A_{2A} AR model was optimized to fit 2-phenylpentenyl-NECA, which is structurally similar to CGS21680, no additional refinement of the receptor binding site was performed. Not surprisingly, the binding mode of CGS21680 at the A_{2A} AR was

* Corresponding author. Tel.: +1 301 496 9024; fax: +1 301 480 8422.

E-mail address: kajacobs@helix.nih.gov (K.A. Jacobson).

found to be similar to the binding mode of 2-phenylpentenyl-NECA and to other agonists of ARs.^{11–15} In particular, His278 (7.43) appeared in proximity to the 2'- and 3'-hydroxyl groups of the ligand (see [Supplementary data](#)). Amino acid residue numbers shown in parentheses correspond to the Ballesteros–Weinstein numbering system that relates its relative position on a particular helix.¹⁶ Thr88 (3.36) and Ser277 (7.42) were involved in H-bonding interactions with the amido group of the *N*-ethylcarboxamido moiety. The *N*⁶-amino group of CGS21680 formed an H-bond with Asn253 (6.55). In addition, the carboxylic oxygen atom of the 2-[4-(2-carboxylethyl)phenylethylamino] moiety of the ligand established an H-bond with Asn145 (EL2), and the phenyl ring of that moiety could be involved in π - π interactions with the aromatic ring of Phe168 (EL2).

After molecular docking of CGS21680 to the A_{2A} AR, a *N*-(2-aminoethyl)-3-(dimethylamino)propanamide chain was attached to the carboxylic group of the ligand to build the ligand **2** ([Fig. 1](#)). To take into account the hydrophobic nature of the methylene groups of PAMAM, a 3-(dimethylamino)propanamide fragment was used instead of a 3-(amino)propanamide moiety. A Monte Carlo Multiple Minimum conformational search analysis (MCM) was utilized to obtain the most favorable conformation and orientation of the ligand inside the A_{2A} AR. The ligand and all residues located within 5 Å around the ligand were subjected to MCM calculations with a shell of constrained residues located within an additional 2 Å. The following parameters were used: MMFFs force field, water as an implicit solvent, maximum of 500 iterations of the Polak-Ribier conjugate gradient (PRCG) minimization method with a convergence threshold of 0.05 kJ mol⁻¹ Å⁻¹, number of conformational search steps = 100, energy window for saving structures = 100 kJ mol⁻¹. The results of MCM calculations indicated that the long chain at the position 2 of the adenine ring of the ligand is oriented toward the extracellular part of the receptor. In particular, in the model obtained the *N*-(2-aminoethyl)-3-(dimethylamino)propanamide moiety was located between the extracellular parts of TM4 and TM5 of the A_{2A} AR. Moreover, the terminal amino group of this chain was found outside the receptor.

The model of the A_{2A} AR with the docked ligand **2** was used to build a model of the A_{2A} AR homodimer, for which physical evidence was reported.^{2b} With this aim, our recently published model of the A₃ AR homodimer was utilized as a template.¹⁷

The A_{2A} AR monomer with the ligand docked inside was duplicated and superimposed with each subunit of the A₃ AR dimer using the Protein Structure Alignment tool implemented in the MacroModel software. Then, the geometry of the A_{2A} AR side chains was optimized by energy minimization in the MMFFs force field. The PRCG minimization method was used. The resulting model of the A_{2A} AR dimer is shown in [Figure 2](#).

The initial model of the A_{2A} AR was built based on the X-ray structure of rhodopsin, and as in rhodopsin, EL2 of the A_{2A} AR covers the binding site to prevent exit of a ligand from the receptor. However, as shown in [Figure 2](#), the *N*-(2-aminoethyl)-3-(dimethylamino)propanamide chain of **2** was located under EL2 and oriented toward the upper parts of TM4 and TM5 in the model. Such an orientation of the ligand **2** allows its *N*-(2-aminoethyl)-3-(dimethylamino)propanamide moiety to be outside the receptor without significant changes in the structure of EL2.

As shown in [Figure 2](#), the terminal amino groups of the ligand **2** located inside the receptor subunits were oriented toward each other. However, the distance between the nitrogen atoms of the amino groups was found to be 11.2 Å. Thus, it is unlikely that the A_{2A} AR dimer subunits can be occupied by CGS21680 units, if they are closest neighbors on one branch of the PAMAM dendrimer. For this reason, the second 3-(dimethylamino)-*N*-ethylpropanamide chain was attached to the terminal nitrogen atoms of the ligands **2** docked to each dimer subunit providing ligand **3**. The length

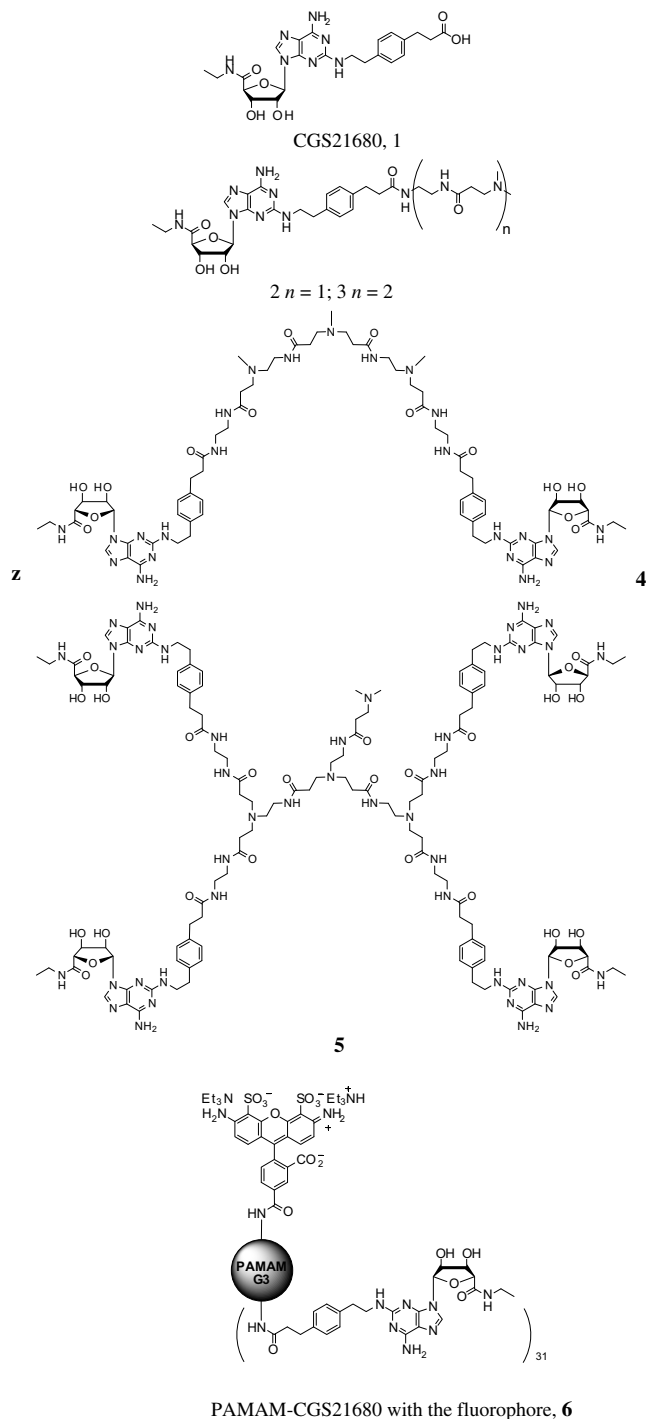


Figure 1. The molecules and conjugates used in molecular docking studies. The entire chemical structure of **6** is provided in [Supplementary data](#).

and flexibility of the poly(amidoamine) chains connected to CGS21680 allowed us to manually adjust the conformation of these chains to superimpose their terminal nitrogen atoms. Then, the terminal nitrogen atom of one ligand was deleted and a remaining terminal ethylene group of this ligand was connected to the terminal nitrogen atom of the second ligand. This resulted in compound **4** bound to the A_{2A} AR dimer. To refine the geometry of the model, the obtained bivalent ligand bound to the A_{2A} AR dimer was subjected to MCM calculations with the same parameters as described above. Then, two additional CGS21680 moieties with



Figure 2. The molecular model of the A_{2A} AR homodimer with the compound **2** inside.

amidoamine chains attached, and an additional 3-(dimethylamino)-*N*-ethylpropanamide fragment were connected to ligand **4** resulting in compound **5** (Fig. 1). The geometry of the model was optimized by energy minimization (Fig. 3).

In parallel to the molecular modeling of the A_{2A} AR dimer, a model of the PAMAM G3 dendrimer was constructed. With this aim, the 3-dimensional structure of the PAMAM generation 0 (G0) was sketched with the MacroModel software and subjected to MCMM calculations. The number of the conformational search steps was set to 500, and the energy window for saving structures

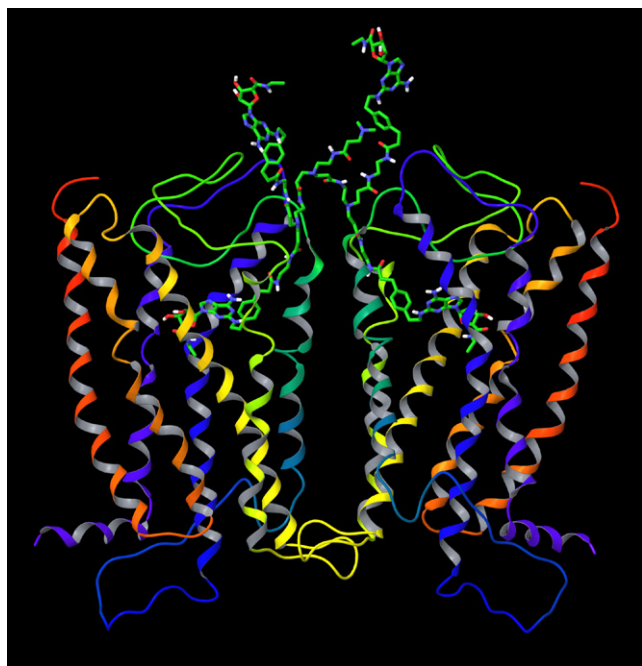


Figure 3. The ligand **5** docked to the A_{2A} AR homodimer.

of 500 kJ mol⁻¹ was used. The resulting model of the G0 dendrimer was used as a starting structure to build a model of the entire PAMAM G3 dendrimer. The PAMAM generations G1, G2, and G3 were obtained by manual attachment of corresponding amidoamine chains to the previous generation followed by optimization of the geometry with MCMM calculations.

The compactness of a polymer structure can be characterized by the value of its radius of gyration. The radius of gyration is calculated as

$$R_g = \left(\frac{\sum_i \|r_i\|^2 m_i}{\sum_i m_i} \right)^{\frac{1}{2}}$$

where m_i is the mass of atom i and r_i is the position of atom i with respect to the center of mass of the molecule. The value of R_g of the PAMAM G3 molecular model obtained after MCMM calculations was calculated with the GROMACS software¹⁸ and was found to be 1.64 nm. The calculated value of R_g is in good agreement with the experimental value of R_g = 1.58 nm measured with the small-angle X-ray scattering (SAXS) method.¹⁹ In order to quantitatively characterize the overall shape of the PAMAM G3 dendrimer the ratio of the principal moments of inertia (I_z/I_x and I_z/I_y) were calculated. I_x , I_y , and I_z represent the eigenvalues of the radius of gyration tensor S , and $I_x \leq I_y \leq I_z$.²⁰ The obtained values of I_z/I_y = 1.5 and I_z/I_x = 1.1 suggested that the model of PAMAM dendrimer has a compact spherical structure. In addition, the value of relative shape anisotropy was calculated as $k^2 = 1 - 3I_2/I_1^2$, where $I_1 = I_x + I_y + I_z$ is the first invariant of S , and $I_2 = I_x I_y + I_y I_z + I_x I_z$ is the second invariant of S . For a linear array of skeletal atoms k^2 = 1, and for structures of high 3-dimensional symmetry k^2 = 0. The value of k^2 calculated for the PAMAM G3 molecular model was found to be k^2 = 0.012 also indicating compact spherical structure of the dendrimer.

Since the model of PAMAM dendrimer obtained after MCMM calculations demonstrated a reasonable size and shape it was used for the conjugation with CGS21680 units. Multiple copies of

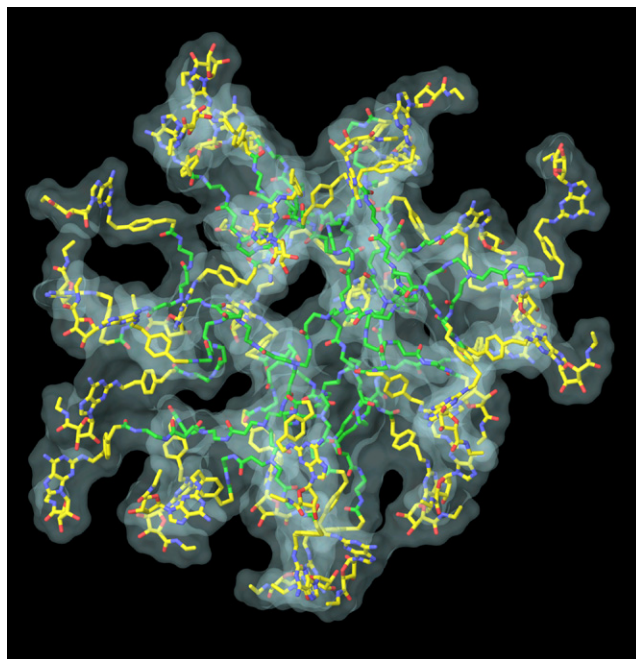


Figure 4. Molecular model of PAMAM-CGS21680 dendrimer obtained after MCMM calculations. The carbon atoms of PAMAM are colored in green, and carbon atoms of CGS21680 units are colored in yellow. Also, the molecular surface of the dendrimer is shown.

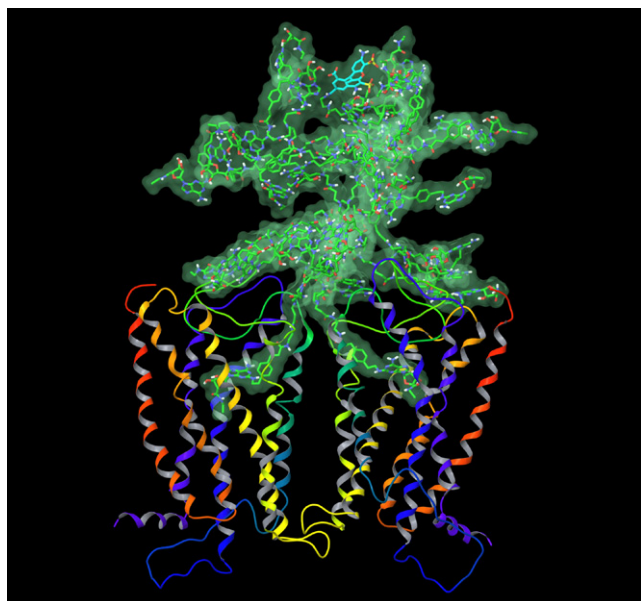


Figure 5. The final model of PAMAM-CGS21680 with the fluorophore, **6** bound to the A_{2A} AR homodimer. The carbon atoms of PAMAM and CGS21680 units are colored in green, carbon atoms of fluorophore are colored in cyan. The distances between the ribose ring oxygens (34.96 Å) and between $C\alpha$ atoms of the N-terminal Met residue of each A_{2A} subunit (66.86 Å) were measured. The overall height of the complex of the receptor dimer with the dendrimer bound is about 110 Å.

CGS21680 moieties were connected to the terminal amino groups of the PAMAM model to build a model of the fully substituted PAMAM-CGS21680. To avoid the overlapping of the CGS21680 units with the amidoamine chains of the dendrimer the initial orientation of CGS21680 moieties was manually adjusted. Then, the model was optimized by a MCMM conformational search analysis (Fig. 4).

In order to combine the models of the A_{2A} AR dimer and PAMAM-CGS21680 dendrimer, the following procedure was performed. A dendron fragment of dendrimer **6**, corresponding to ligand **5** excluding the terminal dimethylamino group was removed from **6**. In turn, the terminal dimethylamino group was removed from ligand **5** in its docked conformation at the A_{2A} AR homodimer. Then, the above-mentioned truncated dendrimer conjugate was connected to the remaining ethylene group of ligand **5**, to complete the structure of **6** docked in the receptor. In the model obtained, several chains of PAMAM-CGS21680 overlapped with the A_{2A} AR structure. The conformation of those chains was manually adjusted, and the model was subjected to the energy minimization. Then, a randomly selected CGS21680 unit was replaced by the fluorophore (Alexa Fluor 488) molecule providing dendrimer **6**. The model geometry was refined by energy minimization followed by 100 ps of molecular dynamics (MD) simulation. The MD simulation was performed with the MacroModel software. The following parameters of the MD simulation were used: force field MMFFs, water as an implicit solvent, a maximum of 500 iterations of the Polak-Ribier conjugate gradient (PRCG) minimization method with a convergence threshold of $0.05 \text{ kJ mol}^{-1} \text{ Å}^{-1}$, SHAKE constraints for all bonds to hydrogen atoms, simulation temperature of 300.0 K, time step of 1.0 fs, equilibration time of 1.0 ps, simulation time of 100.0 ps. The final molecular model of the PAMAM-CGS21680 bound to the A_{2A} AR dimer is shown in Figure 5.

After the MD simulation, the analysis of the binding mode of CGS21680 units located inside the A_{2A} AR dimer was performed. The binding mode of each subunit was found to be similar as

compared with the initial model of CGS21680 docked to the A_{2A} AR and remained in agreement with the data of site-directed mutagenesis.²¹ These results confirmed the principal possibility for the A_{2A} AR homodimer subunits to be occupied at the same time by two CGS21680 units conjugated with the PAMAM G3 dimer.

To summarize, the first molecular model of the A_{2A} AR homodimer has been proposed and utilized for the molecular docking of a potent agonist of the A_{2A} AR, i.e., CGS21680. Molecular models of pure PAMAM G3 dendrimer and PAMAM-CGS21680 have been constructed. The overall shape and size of the PAMAM G3 model was found in good agreement with available experimental data. Molecular model of PAMAM-CGS21680 bound to the A_{2A} AR dimer was proposed for the first time. It was shown that both subunits of the A_{2A} AR dimer can be occupied simultaneously by CGS21680 moieties of the PAMAM-CGS21680 dendrimer. We believe that these results can be useful for further investigation of interactions between GPCRs and dendrimer macromolecules and for the rational design of novel multivalent ligands for ARs and other GPCR homo- and heterodimers.

Acknowledgments

This research was supported by the Intramural Research Program of the NIH, National Institute of Diabetes & Digestive & Kidney Diseases. We thank Athena M. Klutz and Dr. Yoonkyung Kim for helpful discussions.

Supplementary data

The chemical structure of PAMAM-CGS21680 dendrimer and the detailed view of the CGS21680 at the A_{2A} AR monomer. Supplementary data associated with this article can be found in the online version, at [doi:10.1016/j.bmcl.2008.06.087](https://doi.org/10.1016/j.bmcl.2008.06.087).

References and notes

- Chabre, M.; le Maire, M. *Biochemistry* **2005**, *44*, 9395.
- (a) Franco, R.; Casadó, V.; Cortés, A.; Mallol, J.; Ciruela, F.; Ferré, S.; Lluís, C.; Canela, E. *Br. J. Pharmacol.* **2008**, *153*, S90; (b) Canals, M.; Burgueno, J.; Marcellino, D.; Cabello, N.; Canela, E.; Mallol, J.; Agnati, L.; Ferré, S.; Bouvier, M.; Fuxe, K.; Ciruela, F.; Lluís, C.; Franco, R. *J. Neurochem.* **2004**, *88*, 726.
- Maggio, R.; Novi, F.; Scarselli, M.; Corsini, G. U. *FEBS J.* **2005**, *272*, 2939.
- Jacobson, K. A.; Xie, R.; Young, L.; Chang, L.; Liang, B. T. *J. Biol. Chem.* **2000**, *275*, 30272.
- Morphy, R.; Rankovic, Z. *J. Med. Chem.* **2005**, *48*, 6523.
- Messer, W. S., Jr. *Curr. Pharm. Des.* **2004**, *10*, 2015.
- Zhang, A.; Liu, Z.; Kan, Y. *Curr. Top. Med. Chem.* **2007**, *7*, 343.
- Kim, Y.; Hechler, B.; Klutz, A. M.; Gachet, C.; Jacobson, K. A. *Bioconjug. Chem.* **2008**, *19*, 406.
- Glide, version 4.5, Schrödinger, LLC, New York, NY, 2007.
- Kim, S.-K.; Gao, Z.-G.; Van Rompaey, P.; Gross, A. S.; Chen, A.; Van Calenbergh, S.; Jacobson, K. A. *J. Med. Chem.* **2003**, *46*, 4847.
- MacroModel, version 9.5, Schrödinger, LLC, New York, NY, 2007.
- Costanzi, S.; Ivanov, A. A.; Tikhonova, I. G.; Jacobson, K. A. *Front. Drug Des. Discov.* **2007**, *3*, 63.
- Palaniappan, K. K.; Gao, Z. G.; Ivanov, A. A.; Greaves, R.; Adachi, H.; Besada, P.; Kim, H. O.; Kim, A. Y.; Choe, A. A.; Jeong, L. S.; Jacobson, K. A. *Biochemistry* **2007**, *46*, 7437.
- Ivanov, A. A.; Wang, B.; Klutz, A. M.; Chen, V. L.; Gao, Z. G.; Jacobson, K. A. *J. Med. Chem.* **2008**, *51*, 2088.
- Ivanov, A. A.; Palyulin, V. A.; Zefirov, N. S. *J. Mol. Graph. Model.* **2007**, *25*, 740.
- Ballesteros, J. A.; Weinstein, H. *Methods Neurosci.* **1995**, *25*, 366.
- Kim, S.-K.; Jacobson, K. A. *J. Mol. Graph. Model.* **2006**, *25*, 549.
- van der van der Spoel, D.; Lindahl, E.; Hess, B.; Groenhof, G.; Mark, A. E.; Berendsen, H. J. C. *J. Comp. Chem.* **2005**, *26*, 1701.
- Prosa, T. J.; Bauer, B. J.; Amis, E. J.; Tomalia, D. A.; Scherrenberg, R. J. *Polym. Sci. B* **1997**, *35*, 2913.
- Theodorou, D. N.; Suter, U. W. *Macromolecules* **1985**, *18*, 1206.
- Duong, H. T.; Gao, Z. G.; Jacobson, K. A. *Nucleosides Nucleotides Nucleic Acids* **2005**, *24*, 1507.